Chen, K., *et al.*: Numerical Study on the Influence of Platen Super-Heater ...
THERMAL SCIENCE: Year 2021, Vol. 25, No. 2A, pp. 833-843

833

NUMERICAL STUDY ON THE INFLUENCE OF PLATEN SUPER-HEATER ON COMBUSTION CHARACTERISTICS IN A 600 MW TANGENTIALLY FIRED PULVERIZED-COAL BOILER

by

Kai CHEN, Xinfei LIU, and Yao QIN*

ᵃ School of Mechanical Engineering, Xijing University, Xi'an, China

Numerical simulations have been conducted to study combustion characteristics of tangentially fired pulverized-coal boiler. A 600 MW tangentially coal-fired boiler was used for investigating the effect of platen super-heaters on the temperature, species distributions and heat transfer. Two furnace models were established, whose difference lies in modelling super-heaters or not. Results show that modelling platen super-heaters is conducive to precisely predict the temperature, species (CO, CO₂, O₂) and heat flux in the platen zone and has a weak influence on these data in zones below the platen. Modelling platen super-heaters has little influence on the NOₓ prediction. Platen super-heaters obviously decrease heat absorbed by water-wall nearby and affects heat distribution coefficient of furnace.

Key words: *coal combustion, numerical simulation, platen super-heaters*

Introduction

The tangentially fired boiler is commonly used steam generation facility in coal-fired power plant due to the advantage of stability and good fullness of flame in furnace. However, the uneven of flue-gas in a large capacity tangentially boiler is quite large and can lead to local overheating [1]. Moreover, the NOₓ emission from the traditional tangentially fired boiler did not meet the demand of increasing strict regulations against air pollutants [2, 3]. To get over these two shortcomings, many studies have been carried out. In these studies, the numerical simulation was widely employed for predicting combustion characteristics and the NOₓ emission in large capacity tangentially fired boilers over last two decades due to rapid developments in the computer science and steady improvements of the numerical analysis theory. Predictions by numerical simulations helped scholars to investigate the flow field, temperature field and species concentration field, which are difficult to be obtained by in-situ tests. Most studies focused on the NOₓ emission. Some scholars studied uneven of the flue-gas, the heat flux distribution, and slagging. A few studies conceptually designed an oxygen-enriched boiler by numerical simulation. Meanwhile, fundamental work on the turbulence, homogeneous combustion, coal devolatilization, char combustion and radiation modelling, in which coal combustion included is proceeding. Besides, effects of the geometric model were also studied. Park *et al.* [4] studied temperature and heat flux exchange at water-walls by coupling models at the flue-gas side and the water side. Hashimoto and Watanabe [5] studied the furnace scale on heat transfer mechanism of coal particles. All work aimed at preciously predicting combustion characteristics in a utility boiler.

---

* Corresponding author, e-mail: ckworst@gmail.com

834

Chen, K., *et al.*: Numerical Study on the Influence of Platen Super-Heater ...
THERMAL SCIENCE: Year 2021, Vol. 25, No. 2A, pp. 833-843

In numerical investigations, some scholars [6-8] modeled boilers with super-heaters in the upper furnace, and some [9-12] did not. However, nobody has investigated effects of super-heaters on combustion characteristics and NO_x productions in furnace by the numerical simulation comprehensively, although super-heaters absorb much heat in a large capacity boiler (about 1/4 in a 600 MW boiler) and can affect the flow field in the upper furnace,.

In the present study, a 600 MW tangentially coal-fired boiler was used for investigating effects of super-heaters by the numerical simulation. Two furnace models were established, whose difference lies in modelling super-heaters or not. Numerical simulations based on these two furnace models were performed. The flow field, temperature field and species concentration field in furnace were examined. Besides, simulation results were compared with measured data from the utility boiler.

Description of boiler

The configuration and dimensions of the 600 MW tangentially coal-fired boiler is shown in fig. 1. The boiler applies separated over fire air (SOFA) to reduce the NO_x emission. Height of the boiler's furnace is 66.2 m, and horizontal cross-section of the boiler's furnace is rectangular with a width of 19.558 m and a depth of 15.4 m. A total of 24 primary air (PA) nozzles divided into 6 rows, which is numbered from A to F, are installed in four corners of the furnace. One secondary air (SA) nozzle is arranged between every two PA nozzles. Two narrow SA nozzles (AA and FF) are installed in the top and bottom of the burners, respectively. Two close-coupled over-fire air (CCOFA) nozzles and five SOFA nozzles are installed in the top of the combustion zone. As shown in fig. 1, the furnace consists of the ash hopper zone, the combustion zone, the reduction zone, the SOFA zone, the burnout zone, and the platen zone. In
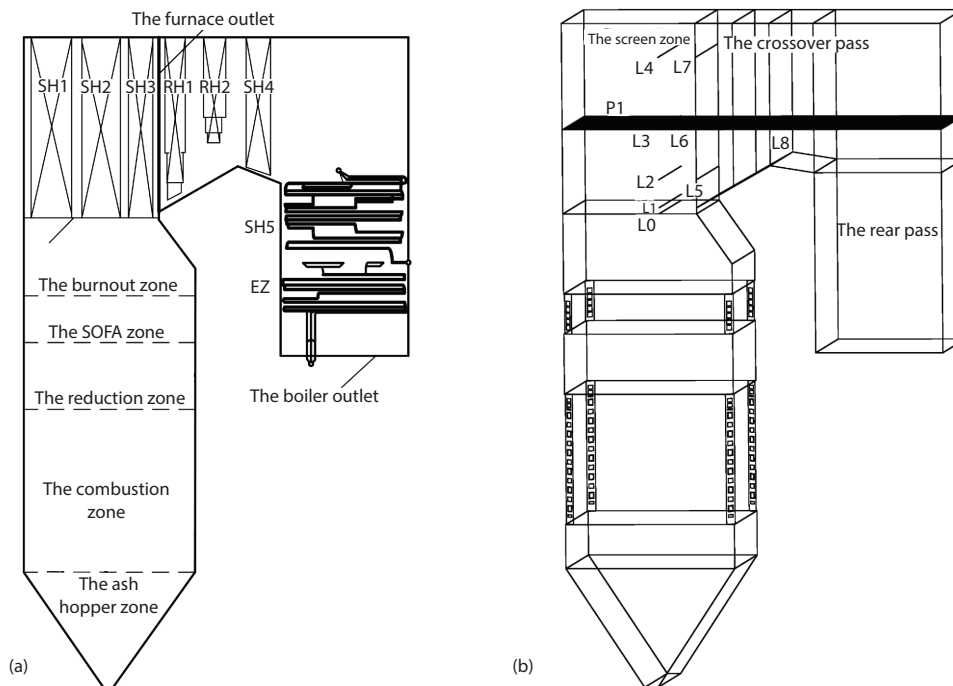

Figure 1. Configuration and dimensions of the 600 MW tangentially coal-fired boiler

the platen zone, there are three groups of platen super-heaters, named as SH1, SH2, and SH3. The SH1 and SH2 have six panels in *Z*-direction, respectively. The spacing between panels is 3048 mm for SH1 and SH2. The SH3 has 25 panels in *Z*-direction and the spacing between panels is 762 mm. More densely arranged bundles following SH3 in the flue-gas-flow direction are named as RH1, RH2, and SH4 in sequence, as shown in fig. 1, where RH is the abbreviation for the re-heater. The SH5 and economizer (EZ) are placed in the rear pass. The horizontal cross-section in furnace at the bottom of super-heaters is named as the platen bottom section. The vertical cross-section in furnace at the right side of SH3 is named as the furnace outlet. The outlet of the rear pass is named as the boiler exit.

Air from SA nozzles, CCOFA nozzles and SOFA nozzles is injected into furnace in horizontal direction. While air from PA nozzles is injected into furnace in both horizontal and vertical directions. Vertical incident angle of air from PA nozzles is 12.4 grids downward. Air from PA nozzles located at four corners is injected into the furnace at set angles. Air from SA nozzles and SOFA nozzles forms contrary imaginary circles to improve uniformity of the flue-gas velocity across the furnace cross-section. Five PA nozzles numbered from A to E are in use and the PA nozzle F is standby. Besides, SOFA nozzles numbered from 2 to 5 are in operation and the SOFA nozzle 1 is standby. Operating information of the 600-MW boiler is shown in tab. 1. Pulverized coal is carried into furnace with the PA equally. A blended coal, comprised of Shenhua coal (80 wt.%) and Baode coal (20 wt.%), is used in the practical operation. R90 of the coal is 18% and the uniformity exponent of the coal is 1.1. The average coal particle size is 55.87 μm.

Table 1. Operating information of the 600-MW boiler

Parameter	Location	Value
Air-flow rates for each nozzle [kgs^{-1}]	PA (nozzle: A, B, C, D, E)	4.84
	SA (nozzle: AB, BC, CD, DE, EF)	10.26
	SA (nozzle: FF)	2.43
	SA (nozzle: AA)	5.68
	SA (perimeter of nozzle: A, B, C, D, E)	3.07
	CCOFA (nozzle: CCOFA-1, CCOFA-2)	8.43
	SOFA (nozzle: SOFA2, SOFA3, SOFA4, SOFA5)	9.36
Air inlet temperature [K]	PA	350
	SA	594
	CCOFA	594
	SOFA	594
Coal mass-flow rate [kgs^{-1}]		62.01
Excess air coefficient		1.2

Numerical simulation

Geometric models

The geometric model without super-heaters is named as No.1 model and the other is named as No.2 model. For No. 2 model, three super-heaters named as SH1, SH2, and SH3 in the upper furnace were modeled as double-sided walls with constant temperature (783 K).

836

Chen, K., *et al.*: Numerical Study on the Influence of Platen Super-Heater ...
THERMAL SCIENCE: Year 2021, Vol. 25, No. 2A, pp. 833-843

The RH1, RH2, SH4, SH5, and EZ were modeled as porous mediums. Inertial resistance coefficients of these heat-absorbing surfaces modeled as porous mediums can be calculated from the measurement data of the pressure drop from the real boiler. However, such measurements were not available for the 600 MW utility boiler in this study. Therefore, inertial resistance coefficients from similar boilers [6, 7] have been used in this study. Detailed inertial resistance coefficients for these heat-absorbing surfaces are shown in tab. 2. Water wall temperatures of both models were set as constant value (650 K).

Table 2. Inertial resistance coefficients of porous mediums

	RH1	RH2	SH4	SH5 and EZ
X-direction	0.72	0.45	0.63	2
Y-direction	0.72	0.45	0.63	2
Z-direction	50	50	50	2

Meshes for the geometric models

Three models with meshes of 1256787 grids, 2346582 grids, and 3764942 grids were built for No. 1 model and three models with meshes of 1409654 grids, 2553079 grids, and 3971439 grids were built for No. 2 model. Under these grid numbers, comparison of flue-gas temperature distributions was done to determine the appropriate gird number. Results indicate that models with meshes of 2346582 grids and 2553079 grids are fine enough to give grid independent solutions for No.1 model and No. 2 model.

Refined meshes were constructed in the regions where a sudden change of the flue-gas velocity is expected, such as regions near each nozzle. The optimized meshes, in which the grid lines are approximately along the flow direction, are constructed in the combustion zone and the SOFA zone. All zones, except the platen zone for No. 2 model, were meshed with structured grids to reduce numerical errors. It should be mentioned that the difference between meshes for the two models lies in the mesh for the platen zone. Structured grids with a total of 260000 grids were used in the mesh for the platen zone for No. 1 model. While unstructured grids with a total of 466497 grids were used in the mesh for the same zone for No. 2 model due to its complex geometries.

Mathematical models

The fluid and particle flow, coal combustion, mass and heat transfer are main phenomena that need to be simulated in furnace. In the present study, standard k-ε model was applied to close turbulent Reynolds equations. Lagrangian method was used for tracing coal particles and stochastic tracking model is used for taking the effect of turbulence on coal particles. One-step model was used for modelling the process that volatile matter releases from coal particles [13]. Kinetics/diffusion-limited model was used for calculating the heterogeneous combustion at the char surface. Probability density function theory was employed to simulate the homogeneous combustion in gas. The discrete ordinates model was used for modelling the radiation heat transfer, thanks to its ability to calculate radiation in narrow space [14]. The NO_x production simulation was carried out as a post-processing procedure after the flow field, temperature distribution, and species concentration in furnace are predicted. These models used in this study just follow in the wake of earlier studies [2, 15]. Default kinetics in Fluent was used, as both trendies of cross-sectional average properties along the furnace and properties at furnace boundaries are not affected by kinetics as these parameters are in reasonable scopes [12].

Chen, K., *et al.*: Numerical Study on the Influence of Platen Super-Heater ...
THERMAL SCIENCE: Year 2021, Vol. 25, No. 2A, pp. 833-843

837

Results and discussion

Calculation validation

Key designed values of the 600 MW boiler were used for validating simulation results. Table 3 shows the validation for both models in detail. The biggest deviation of simulation results from designed values is about 5%, which indicates key data from numerical simulations are in good agreement with the data from designed values. Therefore, simulation results for both models are reliable.

Table 3. Key data from designed values and the numerical simulation results

	Designed values	Simulation results (No. 1 model)	Simulation results (No. 2 model)
Average temperature at the bottom section of the screen [K]	1547	1566.9	1552.9
The O^2 mole fraction at boiler outlet [%]	3.5	3.5	3.5
Heat transfer in SH1and SH2 [MW]	111.7	–	108.0
Heat transfer in SH3 [MW]	126.8	–	100.8

Temperature distributions

Temperature distributions at vertical-cross-section of the boiler for the two models are described in fig. 2(a). It indicates that the highest temperature appears in the combustion zone, and the temperature decreases with the increase of the furnace height. Moreover, the temperature can reach about 2000 K close to the burners, drop to about 1600 K in the central region of the combustion zone. The temperature decreases obviously near the SOFA nozzles since a large amount of the cold SA is injected from SOFA nozzles, and the temperature rises again previous SOFA nozzles due to the combustion of residual combustible. This is in good agreement with early studies [9, 16].

Figure 2(b) shows the cross-sectional average temperature along the furnace height with data from numerical and experimental. It indicates the cross-sectional average temperature from experimental is 100~200 K lower than that obtained by numerical simulations. The reason for this is that experimentally measured temperature is the average temperature of a limited number of points in furnace. Since the temperature across the cross-section has strong non-uni-
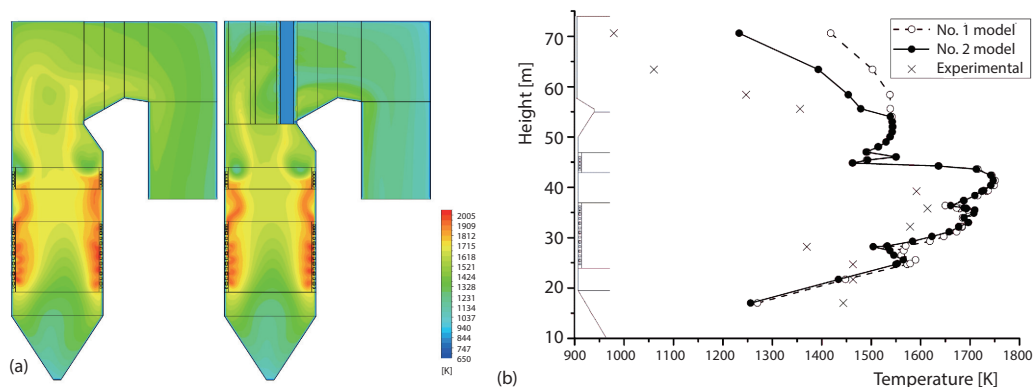

Figure 2. The flue-gas temperature along the furnace height

838

Chen, K., *et al.*: Numerical Study on the Influence of Platen Super-Heater ...
THERMAL SCIENCE: Year 2021, Vol. 25, No. 2A, pp. 833-843

formity, the average temperature from experimental is not exact value of the cross-section. For the same measurement of each cross-section, variations of cross-sectional temperature along the furnace height are believable.

As shown in fig. 2(b), variations of the cross-sectional average temperature along the furnace height obtained by numerical are almost the same as that obtained by experimental. In the upper furnace, variations of the cross-sectional temperature along the furnace height for No. 2 model is closer to that from experiments, as No. 2 model takes platen super-heaters into account. Cross-sectional average temperatures from both models are lower than that from experiments in the ash hopper zone. This may result from combustion models, which underestimates the char combustion in the ash hopper zone.
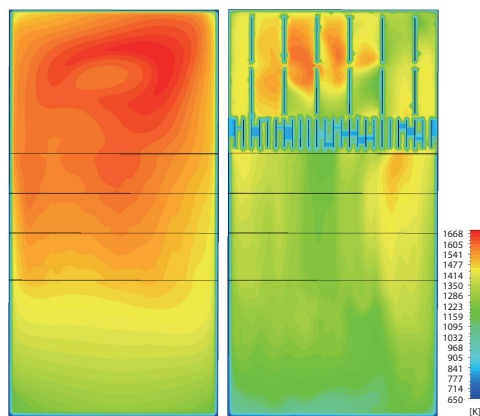

Figure 3. Temperature distributions at P1

The uneven of the flue-gas in the cross-over pass has attracted much attention [6, 7, 17], as it results in tube overheating and rupture. Figure 3 shows temperature distributions for the two models at P1. It shows that the temperature distribution for No. 1 model is much uniform than that for No. 2 model. In addition, the highest temperature at P1 appears at the center of the furnace, and the temperature overall reduces from center to the water wall for No.1 model. However, the temperature distribution for No. 2 model is disorder, which can be attributed to the modelling of platen super-heaters. Since heat-absorbing surfaces of SH1 and SH2 are modeled for No. 2 model, the average temperature for No. 2 model is lower than that for No. 1 model in the cross-over pass, which can be directly observed from fig. 3.

Figure 4 shows flue-gas temperature distributions at L0~L4. It indicates that the flue-gas temperature distribution is successive for No.1 model and sectional successive for No. 2 model [7, 17], as modelling of SH2 decreases the flue-gas temperature nearby. However, rules for distribution of the flue-gas temperature along lines of L0~L4 are still observed in both models. For No. 1 model, the flue-gas temperature firstly increases, then decreases from center to the water wall at lines of L0~L2. The flue-gas temperature at L3 and L4 is essentially constant for No. 1 model. For No. 2 model, the flue-gas temperature firstly increases, then decreases from center to the water wall at lines of L0~L3 and the flue-gas temperature distribution along L4
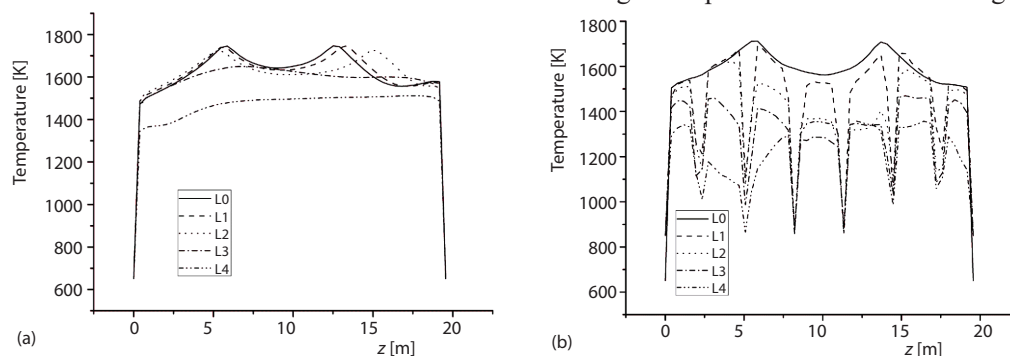

Figure 4. Temperature at the platen zone after SH2 (L ~L4); (a) No. 1 model, (b) No. 2 model

Chen, K., *et al.*: Numerical Study on the Influence of Platen Super-Heater ...
THERMAL SCIENCE: Year 2021, Vol. 25, No. 2A, pp. 833-843

839

presents the opposite rule. At L0, which is below the platen zone, both models show the same flue-gas temperature, which indicates that modelling platen super-heaters does not affect the flue-gas temperature below. The flue-gas temperature at lines of L0~L4 shows that the uneven of the flue-gas temperature for No. 2 model is larger than that for No. 1 model in both vertical and horizontal directions, since super-heaters modeled for No. 2 model change temperature and velocity of the flue-gas in the platen zone.

Figure 5 shows distributions of the flue-gas temperature along lines of L5~L7. It shows that the maximum fluctuation value of the flue-gas temperature at one line can reach 100~200 K for No. 1 model and 200~300 K for No. 2 model, which is in accordance with early studies [4, 7]. For No. 1 model, the flue-gas temperature decreases with the furnace height overall and the flue-gas temperature at the right side is higher than that at the left side [17], which is attributed to the residual swirling of the flue-gas. As the furnace height increases, the residual swirling diminishes, and the maximum fluctuation value of the flue-gas temperature decreases. However, the residual swirling still exists at the furnace outlet, and results in uneven of the flue-gas temperature in the horizontal direction. For No. 2 model, the fluctuation value of the flue-gas temperature reaches the maximum at L6. A sudden drop of the flue-gas temperature is observed in the horizontal direction. The place where the sudden drop of the flue-gas temperature takes place turns from the right side to the left side as the furnace height increases, which can also be explained by the residual swirling of the flue-gas. The difference of the flue-gas temperature at the furnace outlet from the two models is due to super-heaters modeled for No. 2 model. Obviously, the flue-gas temperature for No. 2 model is more convincing, and super-heaters should be modeled in numerical simulations.
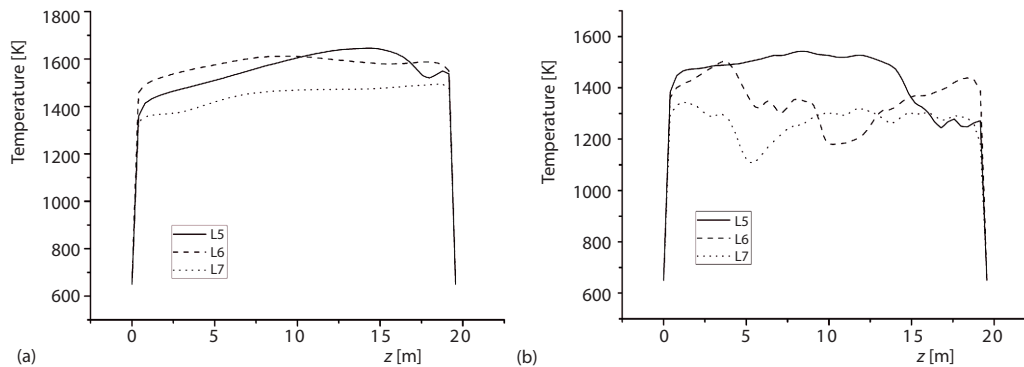

Figure 5. Temperature at the platen zone after SH3 (the furnace outlet) (L5~L7);
(a) No. 1 model, (b) No. 2 model

Uneven of the flue-gas heat flux

The overheating and rupture on tubes, which emerges in the cross-over pass in general, results from the uneven of the flue-gas heat flux, structure and the water heat flux of super-heaters. In this study, the uneven of the flue-gas heat flux in the rear pass is studied and the flue-gas heat flux is defined:

$$q = \rho v_x h \qquad (1)$$

where q [Wm^{-2}] is the heat flux of the flue-gas, ρ [kgm^{-3}] – the density of the flue-gas, v_x [ms^{-1}] – is velocity of the flue-gas in the x-direction, and h [Jkg^{-1}] is sensible enthalpy of the flue-gas.
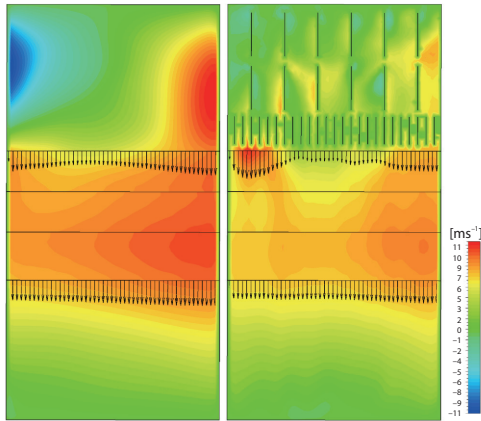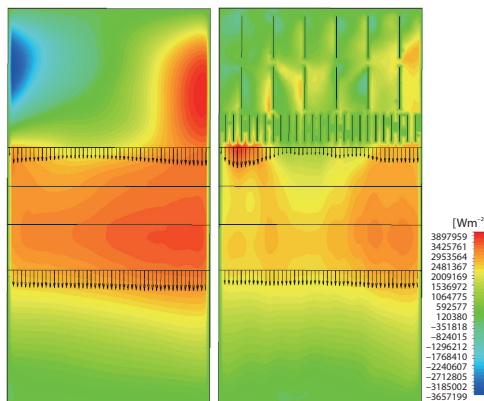
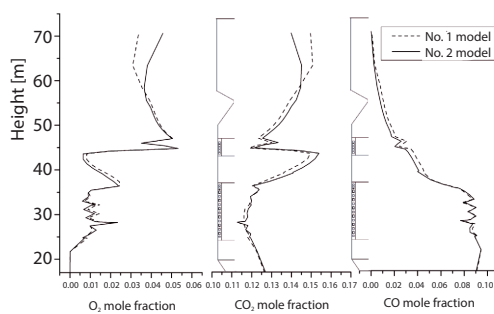**Figure 6. The v_x at P1**

Figure 7. The heat flux of flue-gas at P1

Figure 8. Species distributions along the furnace height

It is shown in eq. (1) that the uneven of the flue-gas density, velocity and temperature are reasons for the uneven of the flue-gas heat flux. As a factor affecting the uneven of the flue-gas heat flux, the velocity in the x direction at P1 is shown in fig. 6. Due to super-heaters modeled for No. 2 model, v_x for No. 2 model is much uniform than that for No. 1 model in the platen zone in the cross-section. However, in the cross-over pass, which is after the furnace outlet, v_x for both models seems to be symmetrical. Moreover, v_x at lines of L6 and L8 is shown in fig. 6. Results from both models show the same rule that v_x decreases from sides to the center at L6, although values of v_x for the two models have slight difference. Since heat-absorbing surfaces have been modeled in the crossover pass, the value of v_x for both models are uniform at L8. These results are in good agreement with early studies [4, 7].

Figure 7 shows the flue-gas heat flux at P1. It indicates that q plays the same rule with v_x at P1. In the platen zone, q for No. 2 model is much uniform than that for No. 1 model. In the crossover pass, q for both models seems to be symmetrical. At L6, q decreases from sides to the center, while q for both models are uniform at L8. As v_x and q show the same rule from sides to the center, it can be concluded that the uneven of velocity is the main reason for the uneven of the flue-gas heat flux.

Species distributions

Figure 8 presents the cross-sectional average mole fraction of O_2, CO_2, and CO along the furnace height. As it can be seen, O_2 is rapidly consumed as it is injected into furnace since O_2 is needed to sustain the combustion. When SOFA is injected into furnace, the O_2 concentration firstly increases, and then decreases gradually with the furnace height. Moreover, it is clear that the residual O_2 for No. 1 model is lower than that for No. 2 model in the platen zone. The reason is that, for No. 1 model, SOFA injected into furnace flows upward near the water wall and is not well mixed with the upward flue-gas. While super-heaters modeled for No. 2 model enhances the mixing of SOFA and upward flue gas to some extent. Figure 8 depicts distributions of the cross-sectional CO_2 mole fraction along the furnace height for the two models. It can be seen that the concentration of CO_2 is in contrast to the concentration of O_2, since in the

Chen, K., *et al.*: Numerical Study on the Influence of Platen Super-Heater ...
THERMAL SCIENCE: Year 2021, Vol. 25, No. 2A, pp. 833-843

841

combustion possess O_2 is consumed and CO_2 is generated. CO concentrations for both models decrease with the furnace height and tend to be zero in the platen zone.

Numerical simulation has been widely used for predicting NO_x concentration. As shown in fig. 9(a), most NO is generated in the combustion zone near burners. The NO distributions in the platen zone and the crossover pass are different as the platen super-heater modeled for No. 2 model affects the mixing of species. Simulation results show that the average NO mole fractions at the boiler exit are 218.64 ppm (6% of O_2) for No.1 model and 198.96 ppm (6% of O_2) for No. 2 model, which have little difference. Figure 9(b) shows volumetric flowrate of NO along the furnace height. A decrease of the NO volumetric flowrate is observed in the upper combustion zone and the reduction zone for both models, since CCOFA and SOFA are designed for NO_x reduction. A decrease of the NO volumetric flowrate is also observed in the platen zone for both models. However, it does not mean NO is reduced in the platen zone, since part of NO in the platen zone flows out of furnace in the horizontal direction and the NO volumetric flowrate presented here is the cross-sectional average in furnace. Figure 9(b) shows that volumetric flowrate of NO for No. 2 model is overall a bit smaller than that for No. 1 model, which may result from the slight difference in temperature and species for the two models. In general, both models can be used for predicting the NO_x emission and the NO_x generation process.
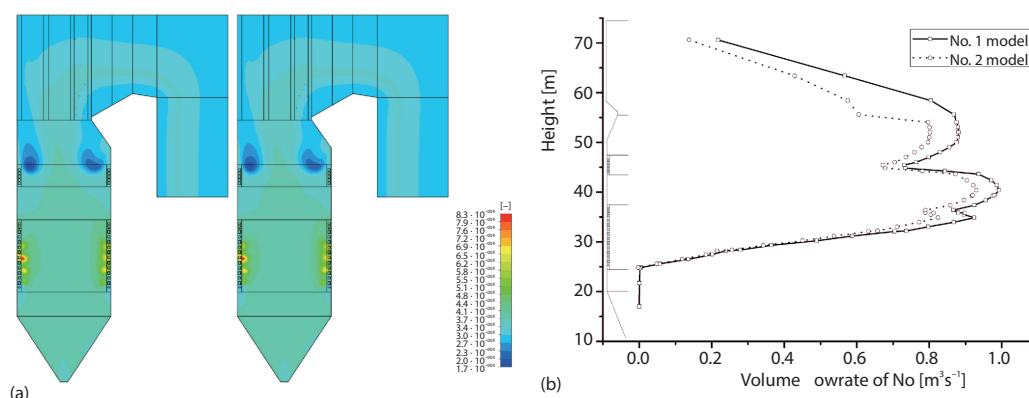

Figure 9. The NO distributions in furnace; (a) mole fraction of NO in furnace, (b) volume flowrate of NO along furnace height

Heat flux distributions

Numerical simulation has been used for predicting the heat flux distribution in furnace of boiler [16, 18-20], which is very important for safe operation of boilers and is hard to be obtained by in-situ tests. Figure 10(a) shows numerical values of the heat flux in each zone for the two models. It indicates that heat flux beneath the platen zone are almost same for the two models, while heat fluxes in the platen zone are different. In the platen zone, the heat flux from No. 2 model is less than half of that from No. 1 model, since the heat exchange between the flue-gas and platen super-heaters for No. 2 model decreases the flue-gas temperature, and the radiation scale length for No. 2 model is less than that for No. 1 model in the platen zone.

Parameters of the heat flux density and the heat distribution coefficient are defined. The heat flux density is defined as the heat exchange flux divided by the area of surface absorbing heat. The heat distribution coefficient is defined as the heat flux density of a heat-absorbing surface in furnace divided by the heat flux density of the whole furnace. The heat distribution
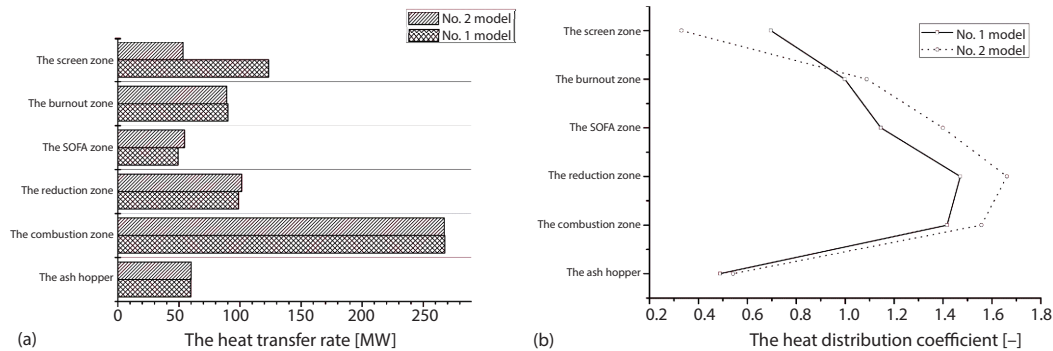
Figure 10. Heat flux distributions for the two models; (a) heat transfer rate, (b) heat distribution coefficient

was extracted from experimental data for calculating the heat flux of some surface in furnace. However, no reliable heat distribution coefficient *was* reported for the tangentially fired pulverized-coal boiler. Numerical simulation offers a method for obtaining the heat distribution coefficient with a small cost. Figure 10(b) shows heat distribution coefficients from the two models. It shows that the heat distribution coefficient for No. 2 model is larger than that for No. 1 model below the platen, although heat flux densities below the platen are almost identical for the two models. The reason for this is that the heat flux density of the whole furnace obtained from No.1 model is larger than that obtained from No. 2 model, due to different heat fluxes for the two models in the platen zone. In the platen zone, the heat distribution coefficient for No. 2 model is almost half of that for No. 1 model, as the heat flux for No. 2 model is less than half of that for No. 1 model. It indicates heat distribution coefficients for the two models have a great difference. Obviously, the data from No. 2 model is more convincing and platen super-heaters should be modeled if the heat distribution coefficient of furnace is studied.

Conclusions

Effect of platen super-heater on combustion characteristics in a 600 MW tangentially fired boiler has been studied numerically. The main conclusions follow.
- Modelling platen super-heaters is conducive to precisely predict the temperature, species (CO, CO_2, and O_2) and heat flux in the platen zone.
- Modelling platen super-heaters has no obvious influence on the NO_x prediction.
- Platen super-heaters obviously decrease heat absorbed by water-wall near the platen zone. When the heat distribution coefficient of furnace is studied, platen super-heaters should be modeled.

References

[1] Zhou, Y., *et al.*, Experimental and Numerical Study on the Flow Fields in upper Furnace for Large-Scale Tangentially Fired Boilers, *Applied Thermal Engineering*, *29* (2009), 4, pp. 732-739
[2] Zhang, J., *et al.*, Optimization of Separated Overfire Air System for a Utility Boiler from a 3-MW Pilot-Scale Facility. *Energy and Fuels*, *27* (2013), 2, pp. 1131-1140
[3] Diez, L.I., *et al.*, Numerical Investigation of NO_x Emissions from a Tangentially-Fired Utility Boiler Under Conventional and Overfire Air Operation, *Fuel*, *87* (2008), 7, pp. 1259-1269
[4] Park, H. Y., *et al.*, Reduction of Main Steam Temperature Deviation in a Tangentially Coal-Fired Two Pass Boiler, *Fuel*, *166* (2016), Feb., pp. 509-516
[5] Hashimoto, N., Watanabe, H., Numerical Analysis on Effect of Furnace Scale on Heat Transfer Mechanism of Coal Particles in Pulverized Coal Combustion Field, *Fuel Processing Technology*, *145* (2016), May, pp. 20-30

Chen, K., *et al.*: Numerical Study on the Influence of Platen Super-Heater ...
THERMAL SCIENCE: Year 2021, Vol. 25, No. 2A, pp. 833-843

843

[6]   Yin, C., *et al.*, Investigation of the Flow, Combustion, Heat Transfer and Emissions from a 609 MW Utility Tangentially Fired Pulverized-Coal Boiler, *Fuel*, *81* (2002), 8, pp. 997-1006
[7]   Yin, C., *et al.*, Further Study of the Gas Temperature Deviation in Large-Scale Tangentially Coal-Fired Boilers, *Fuel*, *82* (2003), 9, pp. 1127-1137
[8]   Park, H. Y., *et al.*, Coupled Fluid Dynamics and Whole Plant Simulation of Coal Combustion in a Tangentially-Fired Boiler, *Fuel*, *89* (2010), 8, pp. 2001-2010
[9]   Zhou, H., *et al.*, Numerical Simulation of the NO_x Emissions in a 1000 MW Tangentially Fired Pulverized-Coal Boiler: Influence of the Multi-Group Arrangement of the Separated over Fire Air, *Energy and Fuels*, *25* (2011), 5, pp. 2004-2012
[10] Zeng, L., *et al.*, Numerical Simulation of Combustion Characteristics and NO_x Emissions in a 300 MWe Utility Boiler with Different Outer Secondary-Air Vane Angles, *Energy and Fuels*, *24* (2010), 10, pp. 5349-5358
[11] Habib, M. A., *et al.*, Thermal and Emission Characteristics in a Tangentially Fired Boiler Model Furnace, *International Journal of Energy Research*, *34* (2010), 13, pp. 1164-1182
[12] Chen, K., *et al.*, Effect of Separated Over-Fire Air on Combustion Performance of a 3 MW Pilot-Scale Facility, *Applied Thermal Engineering*, *108* (2016), Sept., pp. 30-40
[13] Jones, J. M., *et al.*, Modelling NO_x Formation in Coal Particle Combustion at High Temperature: An Investigation of the Devolatilisation Kinetic Factors, *Fuel*, *78* (1999), 10, pp. 1171-1179
[14] Korytnyi, E., *et al.*, Computational Fluid Dynamic Simulations of Coal-Fired Utility Boilers: An Engineering tool, *Fuel*, *88* (2009), 1, pp. 9-18
[15] Liu, H., *et al.*, Effect of Two-Level over-Fire Air on the Combustion and No Emission Characteristics in a 600 MW Wall-Fired Boiler, *Numerical Heat Transfer Part a-Applications*, *68* (2015), 9, pp. 993-1009
[16] Zhang, X., *et al.*, Numerical Investigation of Low NO_x Combustion Strategies in Tangentially-Fired Coal Boilers, *Fuel*, *142* (2015), Feb., pp. 215-221
[17] Tian, D., *et al.*, Influence of Vertical Burner Tilt Angle on the Gas Temperature Deviation in a 700 MW Low NO_x Tangentially Fired Pulverised-Coal Boiler, *Fuel Processing Technology*, *138* (2015), Oct., pp. 616-628
[18] Haryanto, A., Hong, K.S., Modelling and Simulation of an Oxy-Fuel Combustion Boiler System with Flue Gas Re-Circulation, *Computers and Chemical Engineering*, *35* (2011), 1, pp. 25-40
[19] Guo, J., *et al.*, Numerical Investigation on Oxy-Combustion Characteristics of a 200 MWe Tangentially Fired Boiler, *Fuel*, *140* (2015), Jan., pp. 660-668
[20] Liu, H., *et al.*, Modelling the Occurrence and Methods of Eeducing Thermal Deviations of upper Furnace Heating Surfaces in a 1000 MW Dual Circle Tangential Firing Single Furnace Ultra-Supercritical Boiler, *Numerical Heat Transfer Part a-Applications*, *66* (2014), 7, pp. 816-838